Journal Title
XX(X):1–17

DOI: 10.1177/ToBeAssigned
www.sagepub.com/
SAGE

An innovative dynamic observer for nonlinear interconnected systems with uncertainties

Nan Ji[1], Lei Wang[1], Xinggang Yan[2], Dezhi Xu[3]

Abstract

In this paper, an innovative dynamic observer is applied to complex nonlinear interconnected systems with matched and mismatched uncertainties. This dynamic observer can estimate system states, which can not be achieved during the design process for nonlinear interconnected systems with uncertainties. The proposed method has great identification ability with small estimated errors for the states of nonlinear interconnected systems with matched and mismatched uncertainties. It should be pointed out that the considered uncertainties of nonlinear interconnected systems have general forms, which means that the proposed method can be effectively used in more generalised nonlinear interconnected systems. Finally, simulation results for the lateral flight control system are presented to ensure the effectiveness of this strategy.

Keywords

Dynamic observer; nonlinear interconnected systems; matched and mismatched uncertainties, the lateral flight control system.

[1]School of Automation, Wuxi University, Wuxi, 214105, China
[2]School of Engineering and Digital Arts, University of Kent, Canterbury, UK
[3]School of Electrical Engineering, Southeast University, Nanjing, 210096, China

Corresponding author:
Nan Ji, School of Automation, Wuxi University, Wuxi, 214105, China.
Email: jinan1990@foxmail.com

Introduction

In recent years, systems in both industry and daily life have become larger and more complex. They are usually not simple which just has a single function. Most of these complex systems are composed of several subsystems, and all subsystems are interacted with each other (Rtibi et al. (2019); Feydi et al. (2019); Ghali et al. (2020)). This kind of complex systems can be named as interconnected systems. Interconnected systems which widely exist in practical world consist of many subsystems with various functions and structures. For instance, quadrotors, smart cars and electronic monitoring systems are all typical interconnected systems, which are popular in daily life (Attia et al. (2021); Abbasi and Javad (2018); Huong (2023)). Because of nonlinearity, uncertainties, high dimensions and complex components in these interconnected systems, it is very hard to get the accurate values of system states (Trinh et al. (2019)). So, it is difficult to analyse and control the interconnected systems effectively.

In practical application, the states of practical systems are unavailable due to inaccurate modelling or poor operating environment. Many classic control theories based on the accurate values of states in systems can not achieve high performance in this situation. In the case, when system states are not available, one way is to establish an observer to estimate the system states, and then the estimated states are used to form feedback loop if possible (Tlili (2019)). The observer is a kind of dynamic system which is dependent on the inputs and outputs of the original system. With the development of control theory, there are many different kinds of observers which are applied to practical systems, such as unknown input observers, deadbeat observers, SMC observers and backstepping observers etc (Liu (2011); Vafaei and Yazdanpanah (2016); Khalil (2017); Li et al. (2018)). State observers whose convergence rate was faster than the standard asymptotic observers for reaction systems were presented (Ortega et al. (2019)). A sensor-less speed estimator based on an adaptive non-linear high gain observer which only used the measured stator currents and control voltages was presented to estimate the speed of an induction motor (Kadrine et al. (2020)). Event-triggered observers were designed for output-sampled nonlinear state affine systems (Song et al. (2021)). A strategy related to the reduced-order observer of the Boolean control networks for fault diagnosis using the semi-tensor product of matrices was proposed (Zhang et al. (2022)). State estimation using a network of distributed observers with unknown inputs for a class of linear time-invariant systems was presented (Yang et al. (2022)). The output feedback SMC based on dynamic gain observer for an uncertain linear system with unstable zeros was considered (Yeh (2022)). It should be noted that these observers mentioned above are only for general nonlinear control systems and may not applicable to nonlinear interconnected systems.

It is a common situation that states are not available for complex nonlinear interconnected systems. Therefore, the observer is required to identify/estimate state variables for interconnected systems (Chen et al. (2015); Zuo et al. (2023)). In recent years, there are some achievements in this field, but they all have their own limitations to some extent. A full-order nonlinear observer-based control for interconnected power systems was proposed (Mahmud et al. (2012)). The approach of feedback linearisation

was used to design the nonlinear observer when the power system was fully linearised. However, the linearisation of the nonlinear interconnected systems could greatly reduce the accuracy as well as the resulting performance. A novel distributed observer for interconnected multi-rate systems was presented and achieved great results (Orihuela et al. (2017)). But the interconnection of the system was in linear form, which could not be applied to nonlinear form. The new method for designing distributed reduced-order functional observers of a class of interconnected systems with time delays was considered (Trinh and Huong (2018)). In this strategy, interconnected systems without matched uncertainty were not fully nonlinear. Besides that, it had several restrictive conditions due to using the reduced-order observer, but these conditions may not be satisfied in practical applications. Observer-based fuzzy adaptive optimal stabilization control for completely unknown nonlinear interconnected systems was presented (Wang and Tong (2018)). This strategy did not consider the matched uncertainty, and the interconnections had the specific form which needed to satisfy the conditions of fuzzy logic. A decentralised tracking control problem for a class of strict-feedback interconnected systems with unknown parameters was investigated (Guo and Zhang (2021)). This interconnected systems needed to meet several conditions which might not be used in the complex interconnected systems. Based on these reasons above, there are very few excellent research achievements on such complex nonlinear interconnected systems with matched and mismatched uncertainties, and the dynamic observer design for this class of systems is full of challenges and meaningful.

In this paper, the dynamic observer is applied to complex nonlinear interconnected systems in the presence of both matched and mismatched uncertainties. If the uncertain parts are covered by control inputs, this uncertainty is called matched uncertainty; if the parts of uncertainty cannot be completely covered by the control input, this uncertainty can be called mismatched uncertainty. In other words, matched uncertainty is in the direction of the control input, and mismatched uncertainty is not in the direction of the control input, it means that the negative effects of mismatched uncertainty can not be eliminated directly by control input. This dynamic observer can estimate the states which may not be available for control design. The proposed method has great identification ability with small estimated state errors for nonlinear interconnected systems with both matched and mismatched uncertainties. It is pointed out that the uncertainties of nonlinear interconnected systems considered in this paper have general structures, which indicates that the presented strategy can be effectively used in generalised nonlinear interconnected systems with uncertainties, and the full-order observer adopted in this paper reduces the conservatism of the algorithm compared to some results using the reduced-order observer. In the other words, the proposed dynamic observer has several advantages as follows:

1. This dynamic observer is applied to complex nonlinear interconnected systems in the presence of both matched and mismatched uncertainties, many existed results ignored one of them (Trinh and Huong (2018)).
2. The uncertainties of nonlinear interconnected systems considered in this paper are nonlinear and have general structures, which indicates that the presented

strategy can be effectively used in generalised nonlinear interconnected systems with uncertainties. The uncertainties in many existed results are linear or have the specific structure which cannot be applied to general interconnected systems (Mahmud et al. (2012), Orihuela et al. (2017), Guo and Zhang (2021)).

3. This paper adopted the full-order observer which can reduce the conservatism of the algorithm compared to some results using the reduced-order observer. Some results which adopted the reduced-order observer often have more stringent restrictions for the system (Trinh and Huong (2018)), and these restrictions may not be satisfied in practical applications.

The remainder of this paper is organized as follows. Section 'System description and preliminaries' describes the mathematical model of nonlinear interconnected systems with uncertainties and gives some assumptions. Likewise, section 'Dynamic observer design' describes the detailed steps to design a novel dynamic observer for nonlinear interconnected systems with uncertainties. Then, simulation results for a class of practical systems demonstrate the effectiveness of the presented strategy in section 'Simulations for the lateral flight control system'. Finally, the section 'Conclusion' summarizes the entire paper.

System description and preliminaries

Consider a nonlinear interconnected system with uncertainties

$$\dot{x}_i = A_i x_i + B_i(u_i + W_i\sigma_i(x_i,t)) + J_i\kappa_i(x_i,t) + \sum_{j=1}^{n}\Xi_{ij}(x_j,t) \tag{1}$$

$$y_i = C_i x_i, \qquad i = 1,2,\cdots,n \tag{2}$$

where $x_i \in \Gamma_i \subset R^{n_i}$ (Γ_i is a neighbourhood of the origin), $u_i \in R^{m_i}$ and $y_i \in R^{q_i}$ with $m_i \leq q_i < n_i$ are the state, input and output of the $i\text{-}th$ subsystem, respectively. A_i, B_i, C_i, W_i and J_i are known constant matrices with appropriate dimensions. $W_i\sigma_i(x_i,t)$ and $J_i\kappa_i(x_i,t)$ are matched uncertainty and mismatched uncertainty, respectively, where $\sigma_i(x_i,t)$ and $\kappa_i(x_i,t)$ are unknown functions with appropriate dimensions, and the matrices W_i and J_i present the structure of matched and mismatched uncertainties, respectively. $\sum_{j=1}^{n}\Xi_{ij}(x_j,t)$ is the known nonlinear interconnection of the $i\text{-}th$ subsystem. It is assumed that all nonlinear terms involved in this paper are continuous in the considered domain to guarantee the existence of the solutions of the interconnected system (1)-(2).

Assumption 1. *The unknown functions $\kappa_i(x_i,t)$ and $\sigma_i(x_i,t)$ satisfy*

$$\|\kappa_i(x_i,t)\| \leq \eta_i(x_i,t) \tag{3}$$

$$\|\sigma_i(x_i,t)\| \leq \delta_i(x_i,t) \tag{4}$$

where $\eta_i(x_i,t)$ and $\delta_i(x_i,t)$ are known Lipschitz functions with respect to x_i in the domain $\Gamma_i \subset R^{n_i}$ and uniformly about t. The known nonlinear interconnection

$\Xi_{ij}(x_j, t)$ is Lipschitz with respect to x_j in the domain $\Gamma_j \subset R^{n_j}$ and uniformly about t for $i, j = 1, 2, \cdots, n$.

Based on Assumption 1, it follows that for any x_i, $\hat{x}_i$, x_j and $\hat{x}_j$ in the considered domain,

$$\|\eta_i(x_i, t) - \eta_i(\hat{x}_i, t)\| \leq \mathcal{L}_{\eta_i}(t)\|x_i - \hat{x}_i\| \tag{5}$$

$$\|\delta_i(x_i, t) - \delta_i(\hat{x}_i, t)\| \leq \mathcal{L}_{\delta_i}(t)\|x_i - \hat{x}_i\| \tag{6}$$

$$\|\Xi_{ij}(x_j, t) - \Xi_{ij}(\hat{x}_j, t)\| \leq \mathcal{L}_{\Xi_{ij}}(t)\|x_j - \hat{x}_j\| \tag{7}$$

where $\mathcal{L}_{\eta_i}(t)$, $\mathcal{L}_{\delta_i}(t)$ and $\mathcal{L}_{\Xi_{ij}}(t)$ are nonnegative functions in $R^+ = \{t | t \geq 0\}$.

Remark 1. The matrices W_i and J_i are employed to describe the structural characteristics of the nonlinear matched and mismatched uncertainties, respectively. $\sigma_i(x_i, t)$ and $\kappa_i(x_i, t)$ are unknown functions with known bounds which will be used in analysis and observer design later. The specific values of uncertainties may be difficultly achieved, but based on practical experience and data statistics, the approximate bounds of uncertainties can generally be obtained. This situation is very consistent with the practical application of nonlinear interconnected systems with uncertainties.

Assumption 2. *The matrix pair (A_i, C_i) is observable for $i = 1, 2, \cdots, n$.*

Assumption 2 is a basic limitation for the matrix pair (A_i, C_i). An innovative dynamic observer is to be designed in next part.

Dynamic observer design

In view of the observability of the pair (A_i, C_i) in Assumption 2, there exists a matrix L_i such that $(A_i - L_i C_i)$ is stable and thus for any $Q_i > 0$ the following Lyapunov equation has a unique solution $P_i > 0$,

$$(A_i - L_i C_i)^T P_i + P_i(A_i - L_i C_i) = -Q_i \tag{8}$$

Assumption 3. *Known matrices N_i, S_i and P_i exist such that $[J_i \quad B_i W_i]^T P_i = [N_i \quad S_i] C_i$ holds, where P_i satisfies (8), and the matrices B_i, C_i, W_i and J_i are given in the interconnected system (1)-(2).*

Consider the following dynamic system

$$\dot{\hat{x}}_i = A_i \hat{x}_i + B_i(u_i + \Phi_i(\hat{x}_i, y_i, t)) + L_i(y_i - C_i \hat{x}_i) + \Omega_i(\hat{x}_i, y_i, t) + \sum_{j=1}^{n} \Xi_{ij}(\hat{x}_j, t) \tag{9}$$

where $\hat{x}_i \in R^{n_i}$, $L_i \in R^{n_i \times q_i}$ satisfy (8), and

$$\Omega_i(\hat{x}_i, y_i, t) = \begin{cases} J_i \dfrac{N_i(y_i - C_i \hat{x}_i)}{\|N_i(y_i - C_i \hat{x}_i)\|} \eta_i(\hat{x}_i, t), & N_i(y_i - C_i \hat{x}_i) \neq 0 \qquad (10) \\ 0, & N_i(y_i - C_i \hat{x}_i) = 0 \qquad (11) \end{cases}$$

$$\Phi_i(\hat{x}_i, y_i, t) = \begin{cases} W_i \dfrac{S_i(y_i - C_i\hat{x}_i)}{\|S_i(y_i - C_i\hat{x}_i)\|}\delta_i(\hat{x}_i, t), & S_i(y_i - C_i\hat{x}_i) \neq 0 \quad (12) \\ 0, & S_i(y_i - C_i\hat{x}_i) = 0 \quad (13) \end{cases}$$

where matrices J_i, N_i, W_i and S_i satisfy Assumption 3, the known functions $\eta_i(\cdot)$ and $\delta_i(\cdot)$ are given in Assumption 1.

Let state estimated error $e_i = x_i - \hat{x}_i$. It follows from (1) and (9) that the error dynamic is given by

$$\begin{aligned} \dot{e}_i =& (A_i - L_iC_i)e_i + (J_i\kappa_i(x_i, t) - \Omega_i(\hat{x}_i, y_i, t)) + B_i(W_i\sigma_i(x_i, t) - \Phi_i(\hat{x}_i, y_i, t)) \\ &+ \sum_{j=1}^{n}(\Xi_{ij}(x_j, t) - \Xi_{ij}(\hat{x}_j, t)) \end{aligned} \tag{14}$$

The following results are presented to underpin subsequent analysis.

Lemma 1. *Suppose that Assumptions 1-3 are satisfied, the following results hold:*
(i) $e_i^T P_i(J_i\kappa_i(x_i, t) - \Omega_i(\hat{x}_i, y_i, t)) \leq \mathcal{L}_{\eta_i}(t)\|N_iC_i\|\|e_i\|^2$
(ii) $e_i^T P_i B_i(W_i\sigma_i(x_i, t) - \Phi_i(\hat{x}_i, y_i, t)) \leq \mathcal{L}_{\delta_i}(t)\|S_iC_i\|\|e_i\|^2$
(iii) $e_i^T P_i \sum_{j=1}^{n}(\Xi_{ij}(x_j, t) - \Xi_{ij}(\hat{x}_j, t)) \leq \sum_{j=1}^{n} \bar{\lambda}(P_i)\mathcal{L}_{\Xi_{ij}}(t)\|e_j\|\|e_i\|$
where $\mathcal{L}_{\eta_i}(t)$, $\mathcal{L}_{\delta_i}(t)$ *and* $\mathcal{L}_{\Xi_{ij}}(t)$ *are satisfied (5), (6) and (7), respectively.* $\bar{\lambda}(P_i)$ *is the maximum eigenvalue of the matrix* P_i.

Proof. From Assumptions 1 and 3, combining with equations (10) and (11), if $N_iC_ie_i \neq 0$,

$$\begin{aligned} & e_i^T P_i(J_i\kappa_i(x_i, t) - \Omega_i(\hat{x}_i, y_i, t)) \\ &= (N_iC_ie_i)^T\kappa_i(x_i, t) - \frac{(N_iC_ie_i)^T N_iC_ie_i}{\|N_iC_ie_i\|}\eta_i(\hat{x}_i, t) \\ &\leq \|N_iC_ie_i\|\eta_i(x_i, t) - \|N_iC_ie_i\|\eta_i(\hat{x}_i, t) \\ &\leq \mathcal{L}_{\eta_i}(t)\|N_iC_i\|\|e_i\|^2 \end{aligned} \tag{15}$$

Otherwise if $N_iC_ie_i = 0$, then from $J_i^T P_i = N_iC_i$ in Assumption 3, there is

$$e_i^T P_i J_i = (J_i^T P_i e_i)^T = (N_iC_ie_i)^T = 0 \tag{16}$$

Therefore, from analysis above,

$$e_i^T P_i(J_i\kappa_i(x_i, t) - \Omega_i(\hat{x}_i, y_i, t)) \leq \mathcal{L}_{\eta_i}(t)\|N_iC_i\|\|e_i\|^2 \tag{17}$$

Hence the conclusion (i) follows.

From Assumptions 1 and 3, combining with the equations (12) and (13), if $S_iC_ie_i \neq 0$,

$$\begin{aligned} & e_i^T P_i B_i (W_i \sigma_i(x_i,t) - \Phi_i(\hat{x}_i, y_i, t)) \\ & = (S_iC_ie_i)^T \sigma_i(x_i,t) - \frac{(S_iC_ie_i)^T S_iC_ie_i}{\|S_iC_ie_i\|} \delta_i(\hat{x}_i,t) \\ & \leq \|S_iC_ie_i\| \delta_i(x_i,t) - \|S_iC_ie_i\| \delta_i(\hat{x}_i,t) \\ & \leq \mathcal{L}_{\delta_i}(t) \|S_iC_i\| \|e_i\|^2 \end{aligned} \tag{18}$$

Otherwise if $S_iC_ie_i = 0$, then from $(B_iW_i)^T P_i = S_iC_i$ in Assumption 3, there is

$$e_i^T P_i B_i W_i = ((B_iW_i)^T P_i e_i)^T = (S_iC_ie_i)^T = 0 \tag{19}$$

Therefore, from analysis above,

$$e_i^T P_i B_i (W_i \sigma_i(x_i,t) - \Phi_i(\hat{x}_i, y_i, t)) \leq \mathcal{L}_{\delta_i}(t) \|S_iC_i\| \|e_i\|^2 \tag{20}$$

Hence the conclusion (ii) follows.

Based on (7), it follows

$$\begin{aligned} & e_i^T P_i \sum_{j=1}^{n} (\Xi_{ij}(x_j,t) - \Xi_{ij}(\hat{x}_j,t)) \\ & \leq \|e_i\| \bar{\lambda}(P_i) \sum_{j=1}^{n} (\mathcal{L}_{\Xi_{ij}}(t) \|x_j - \hat{x}_j\|) \\ & = \sum_{j=1}^{n} \bar{\lambda}(P_i) \mathcal{L}_{\Xi_{ij}}(t) \|e_j\| \|e_i\| \end{aligned} \tag{21}$$

Hence conclusion (iii) follows.

Theorem 1. *Suppose that Assumptions 1-3 are satisfied. Then, there exists positive constants β_1 and β_2 such that*

$$\|e_i\| \leq \beta_2 exp\{-\beta_1 t\} \tag{22}$$

if $(\Upsilon + \Upsilon^T)$ is positive definite with $\Upsilon = (\upsilon_{ij})_{n\times n}$ defined by

$$\upsilon_{ij} = \begin{cases} \underline{\lambda}(Q_i) - 2\mathcal{L}_{\eta_i}(t)\|N_iC_i\| - 2\mathcal{L}_{\delta_i}(t)\|S_iC_i\| - 2\overline{\lambda}(P_i)\mathcal{L}_{\Xi_{ij}}(t), i = j & (23) \\ -2\overline{\lambda}(P_i)\mathcal{L}_{\Xi_{ij}}(t), \qquad i \neq j & (24) \end{cases}$$

where Q_i is satisfied in equation (8), N_i and S_i are defined in Assumption 3. $\underline{\lambda}(Q_i)$ is the minimum eigenvalue of the matrix Q_i, $\overline{\lambda}(P_i)$ is the maximum eigenvalue of the matrix P_i.

Proof. For the system (14), consider a Lyapunov function candidate $V_1 = \sum_{i=1}^{n} e_i^T P_i e_i$. Then, the time derivative of V_1 along the trajectories of system (14) is given by

$$\dot{V}_1 = \sum_{i=1}^{n} \Big(- e_i^T Q_i e_i + 2e_i^T P_i (J_i \kappa_i(x_i,t) - \Omega_i(\hat{x}_i, y_i, t)) + 2e_i^T P_i B_i (W_i \sigma_i(x_i,t) - \Phi_i(\hat{x}_i, y_i, t)) + 2e_i^T P_i \sum_{j=1}^{n} (\Xi_{ij}(x_j,t) - \Xi_{ij}(\hat{x}_j,t)) \Big)$$

where equation (8) is used above. From conclusions (i)-(iii) of Lemma 1, it follows that

$$\begin{aligned}
\dot{V}_1 \leq & \sum_{i=1}^{n} (-\underline{\lambda}(Q_i)\|e_i\|^2 + 2\mathcal{L}_{\eta_i}(t)\|N_i C_i\|\|e_i\|^2 \\
& + 2\mathcal{L}_{\delta_i}(t)\|S_i C_i\|\|e_i\|^2 + 2\sum_{j=1}^{n} \bar{\lambda}(P_i)\mathcal{L}_{\Xi_{ij}}(t)\|e_i\|\|e_j\|) \\
= & -\sum_{i=1}^{n} (\underline{\lambda}(Q_i) - 2\mathcal{L}_{\eta_i}(t)\|N_i C_i\| - 2\mathcal{L}_{\delta_i}(t)\|S_i C_i\| - 2\overline{\lambda}(P_i)\mathcal{L}_{\Xi_{ij}}(t))\|e_i\|^2 \\
& + \sum_{i=1}^{n} \sum_{j=1, j\neq i}^{n} 2\overline{\lambda}(P_i)\mathcal{L}_{\Xi_{ij}}(t)\|e_i\|\|e_j\| \\
= & -\frac{1}{2}[\|e_1\|\|e_2\| \ldots \|e_n\|](\Upsilon + \Upsilon^T)[\|e_1\|\|e_2\| \ldots \|e_n\|]^T \\
\leq & -\frac{1}{2}\underline{\lambda}(\Upsilon + \Upsilon^T) \sum_{i=1}^{n} \|e_i\|^2
\end{aligned} \tag{25}$$

Given that

$$\sum_{i=1}^{n} e_i^T P_i e_i \leq \max_i\{\overline{\lambda}(P_i)\} \sum_{i=1}^{n} \|e_i\|^2 \tag{26}$$

then, according to (25) and (26), it follows that

$$\begin{aligned}
\dot{V}_1 \leq & -\frac{\underline{\lambda}(\Upsilon + \Upsilon^T)}{2\max_i\{\overline{\lambda}(P_i)\}} \sum_{i=1}^{n} e_i^T P_i e_i \\
= & -\frac{\underline{\lambda}(\Upsilon + \Upsilon^T)}{2\max_i\{\overline{\lambda}(P_i)\}} V_1 \\
= & -2\beta_1 V_1
\end{aligned}$$

where

$$\beta_1 \equiv: \frac{\underline{\lambda}(\Upsilon + \Upsilon^T)}{4\max_i\{\overline{\lambda}(P_i)\}} > 0 \tag{27}$$

Based on the analysis above, it follows that

$$V_1(t) \leq V_1(0)\exp\{-2\beta_1 t\}$$

Since $\min_i\{\underline{\lambda}(P_i)\}\|e_i\|^2 \leq e_i^T P_i e_i \leq \sum_{i=1}^n e_i^T P_i e_i = V_1$, the conclusion $\|e_i\| \leq \beta_2 \exp\{-\beta_1 t\}$ follows by letting

$$\beta_2 > \sqrt{V_1(0)/\min_i\{\underline{\lambda}(P_i)\}} \tag{28}$$

Hence, the result is obtained.

Remark 2. Theorem 1 shows that the dynamic observer in (9) is an exponential observer for the interconnected system (1)-(2). This can be seen from the inequality (22). The proof is also constructive and provides a method to determine the values of β_1 and β_2.

Simulations for the lateral flight control system

Consider a lateral flight control system, which is widely used in civil airliners. The nominal aircraft lateral mode at the cruising flight condition can be presented as (see Wu et al. (1998); Unal (2021))

$$\begin{aligned}\dot{x_1} = &\begin{bmatrix}-1.588 & 0 & -0.883\\ 1 & 0 & 0\\ 0 & 0 & -25\end{bmatrix}\begin{bmatrix}x_{11}\\ x_{12}\\ x_{13}\end{bmatrix}\\ &+\begin{bmatrix}0\\ 0\\ 25\end{bmatrix}(u_1+\sigma_1)+\begin{bmatrix}-0.2164 & -0.1625\\ 1 & 0.75\\ 2 & 1.4\end{bmatrix}\kappa_1(x_1,t)\\ &+\begin{bmatrix}0.07x_{21}+0.045x_{22}+0.037x_{24}\\ 0\\ 0\end{bmatrix}\end{aligned} \tag{29}$$

$$y_1 = \begin{bmatrix}0 & 1 & 0\\ 0 & 0 & 1\end{bmatrix}\begin{bmatrix}x_{11}\\ x_{12}\\ x_{13}\end{bmatrix} \tag{30}$$

$$\begin{aligned}\dot{x_2} = &\begin{bmatrix}-0.161 & 1 & 0 & -0.052\\ -5.446 & -0.386 & 0 & -2.185\\ -5.446 & -0.386 & -0.5 & -2.185\\ 0 & 0 & 0 & -20\end{bmatrix}\begin{bmatrix}x_{21}\\ x_{22}\\ x_{23}\\ x_{24}\end{bmatrix}\\ &+\begin{bmatrix}0\\ 0\\ 0\\ 20\end{bmatrix}u_2+\begin{bmatrix}1 & 0.4\\ -3.685 & -1.474\\ -5.741 & -2.2964\\ 1.2 & 1.9\end{bmatrix}\kappa_2(x_2,t)+\begin{bmatrix}0.02x_{11}+0.01x_{12}\\ 0.01x_{11}\\ 0.01x_{11}\\ 0\end{bmatrix}\end{aligned} \tag{31}$$

$$y_2 = \begin{bmatrix}0 & 0 & 1 & 0\\ 0 & 0 & 0 & 1\end{bmatrix}\begin{bmatrix}x_{21}\\ x_{22}\\ x_{23}\\ x_{24}\end{bmatrix} \tag{32}$$

where $x_1 = \text{col}(x_{11}, x_{12}, x_{13})$ and $x_2 = \text{col}(x_{21}, x_{22}, x_{23}, x_{24})$ denote roll rate, bank angle, aileron deflection, sideslip angle, yaw rate, washout filter output and rudder

deflection, respectively. It is assumed that bank angle, aileron deflection, washout filter output and rudder deflection are available which take as the outputs of the system (29)-(32). Input signals u_1 and u_2 are the perturbed aileron deflection command and the perturbed rudder deflection command, respectively. The dynamic coefficients represent a Boeing 707 aircraft cruising at the specific speed (Wu et al. (1998); Unal (2021)). The uncertainties are assumed to satisfy

$$\|\kappa_1(\cdot)\| \leq \eta_1(\cdot) = 0.045(\sin(x_{11}) + \|x_{12}\|) \tag{33}$$
$$\|\kappa_2(\cdot)\| \leq \eta_2(\cdot) = 0.02(\sin(x_{21}) + \sin(x_{22}) + \|x_{23}\|) \tag{34}$$
$$\|\sigma_1(\cdot)\| \leq \delta_1(\cdot) = 0.08\sin(x_{11}) \tag{35}$$
$$\mathcal{L}_{\eta_1}(\cdot) = 0.09 \tag{36}$$
$$\mathcal{L}_{\eta_2}(\cdot) = 0.06 \tag{37}$$
$$\mathcal{L}_{\delta_1}(\cdot) = 0.13 \tag{38}$$

and

$$\mathcal{L}_{\Xi_{1j}}(\cdot) = 0.2 \tag{39}$$
$$\mathcal{L}_{\Xi_{2j}}(\cdot) = 0.07 \tag{40}$$

where

$$\Xi_{1j}(\cdot) = \begin{bmatrix} 0.07x_{21} + 0.045x_{22} + 0.037x_{24} \\ 0 \\ 0 \end{bmatrix} \tag{41}$$
$$\Xi_{2j}(\cdot) = \begin{bmatrix} 0.02x_{11} + 0.01x_{12} \\ 0.01x_{11} \\ 0.01x_{11} \\ 0 \end{bmatrix} \tag{42}$$

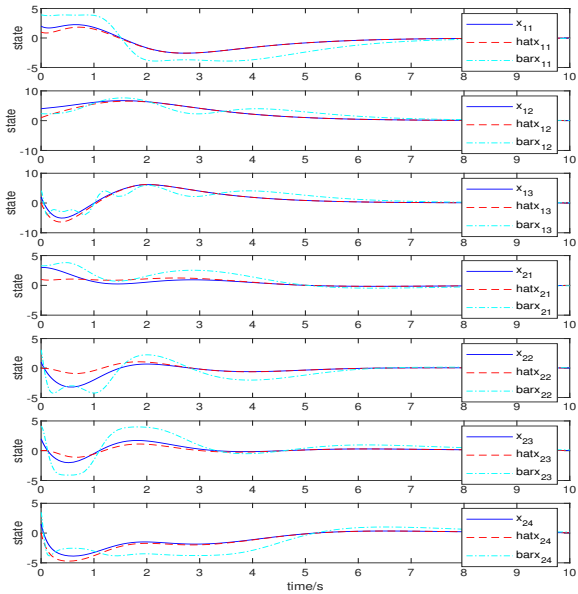

Figure 1. Time responses of the estimated states of the lateral flight control system.

In the lateral flight control system (29)-(32),

$$A_1 = \begin{bmatrix} -1.588 & 0 & -0.883 \\ 1 & 0 & 0 \\ 0 & 0 & -25 \end{bmatrix} \tag{43}$$

$$A_2 = \begin{bmatrix} -0.161 & 1 & 0 & -0.052 \\ -5.446 & -0.386 & 0 & -2.185 \\ -5.446 & -0.386 & -0.5 & -2.185 \\ 0 & 0 & 0 & -20 \end{bmatrix} \tag{44}$$

$$B_1 = \begin{bmatrix} 0 \\ 0 \\ 25 \end{bmatrix} \tag{45}$$

$$B_2 = \begin{bmatrix} 0 \\ 0 \\ 0 \\ 20 \end{bmatrix} \tag{46}$$

$$C_1 = \begin{bmatrix} 0 & 1 & 0 \\ 0 & 0 & 1 \end{bmatrix} \tag{47}$$

$$C_2 = \begin{bmatrix} 0 & 0 & 1 & 0 \\ 0 & 0 & 0 & 1 \end{bmatrix} \tag{48}$$

By direct verification, (A_1, C_1) and (A_2, C_2) are observable, thus Assumption 2 is satisfied.

Choose

$$L_1 = \begin{bmatrix} -0.0363 & -0.8830 \\ 1.9120 & 0 \\ 0 & -24.0000 \end{bmatrix} \tag{49}$$

$$L_2 = \begin{bmatrix} -0.8884 & -0.0520 \\ 4.0914 & -2.1850 \\ 4.9530 & -2.1850 \\ 0 & -19.0000 \end{bmatrix} \tag{50}$$

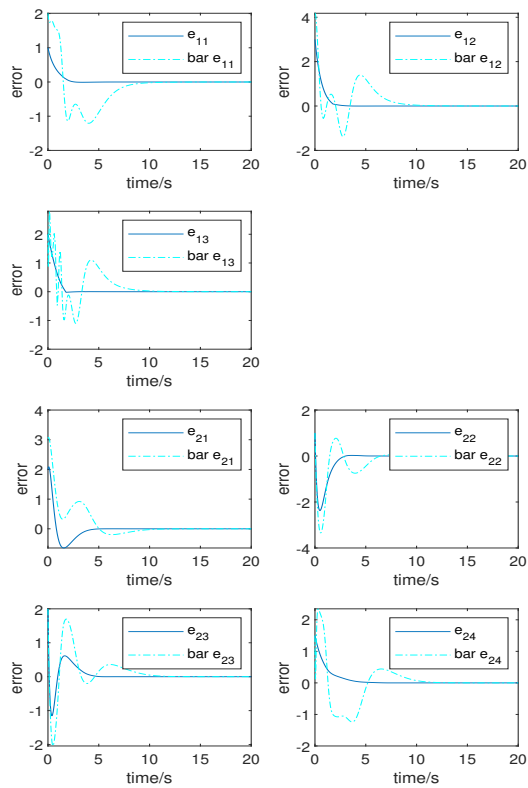

Figure 2. Time responses of observation errors of the lateral flight control system.

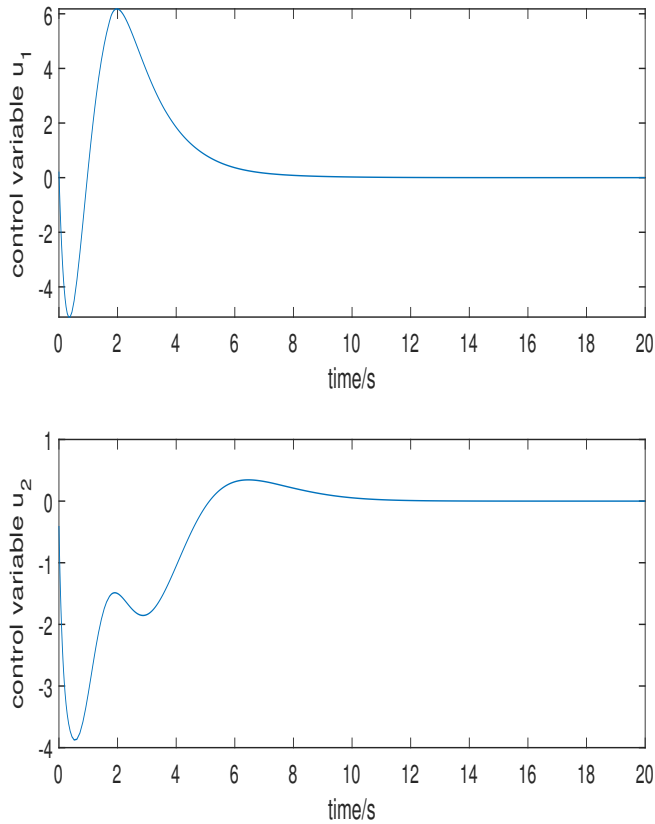

Figure 3. Time responses of control laws of the lateral flight control system.

By calculation, $(A_1 - L_1C_1)$ and $(A_2 - L_2C_2)$ are stable. For $Q_1 = \mathrm{I}_3$ and $Q_2 = \mathrm{I}_4$, the solutions of Lyapunov equation (8) are

$$P_1 = \begin{bmatrix} 0.3646 & 0.0789 & 0 \\ 0.0789 & 0.2630 & 0 \\ 0 & 0 & 0.5000 \end{bmatrix} \tag{51}$$

$$P_2 = \begin{bmatrix} 1.1772 & -0.4134 & 0.4704 & 0 \\ -0.4134 & 0.8277 & -0.6033 & 0 \\ 0.4704 & -0.6033 & 0.6210 & 0 \\ 0 & 0 & 0 & 0.5000 \end{bmatrix} \tag{52}$$

Let

$$J_1 = \begin{bmatrix} -0.2164 & -0.1625 \\ 1 & 0.75 \\ 2 & 1.4 \end{bmatrix} \tag{53}$$

$$N_1 = \begin{bmatrix} 0.2459 & 1 \\ 0.1844 & 0.7 \end{bmatrix} \tag{54}$$

$$W_1 = I \tag{55}$$

$$S_1 = \begin{bmatrix} 0 & 12.5 \end{bmatrix} \tag{56}$$

$$J_2 = \begin{bmatrix} 1 & 0.4 \\ -3.685 & -1.474 \\ -5.741 & -2.2964 \\ 1.2 & 1.9 \end{bmatrix} \tag{57}$$

$$N_2 = \begin{bmatrix} -0.8716 & 0.6 \\ -0.3486 & 0.95 \end{bmatrix} \tag{58}$$

According to (23)-(24),

$$(\Upsilon + \Upsilon^T) = \begin{bmatrix} 1.1468 & -0.4637 \\ -0.4637 & 1.1378 \end{bmatrix} \tag{59}$$

where $(\Upsilon + \Upsilon^T)$ is positive definite, thus Theorem 1 is satisfied. Based on (27) and (28), $\beta_1 = 0.09$ and $\beta_2 = 0.3$.

Then, choose the control law for simulation as follows

$$u_1 = -(-0.0850\hat{x}_{11} - 0.1359\hat{x}_{12} - 0.8835\hat{x}_{13}) \tag{60}$$

$$u_2 = -(0.4032\hat{x}_{21} + 0.0057\hat{x}_{22} - 0.1465\hat{x}_{23} - 0.7024\hat{x}_{24}) \tag{61}$$

The initial values of simulation are selected as $x_1 = \text{col}(2, 4, 2)$, $x_2 = \text{col}(3, 1, 2, 1.5)$, $\hat{x}_1 = \text{col}(1, 1, 0)$ and $\hat{x}_2 = \text{col}(1, 0, 0, 0)$. $\kappa_1(\cdot)$, $\kappa_2(\cdot)$ and $\sigma_1(\cdot)$ are selected as

$$\kappa_1(\cdot) = 0.0112(\sin(x_{11}) + \|x_{12}\|) \tag{62}$$

$$\kappa_2(\cdot) = 0.005(\sin(x_{21}) + \sin(x_{22}) + \|x_{23}\|) \tag{63}$$

$$\sigma_1(\cdot) = 0.04\sin(x_{11}) \tag{64}$$

Fig 1 describes the time responses of the estimated states of the lateral flight control system. It should be noted that $\bar{x} = \text{col}(\bar{x}_{11}, \bar{x}_{12}, \bar{x}_{13}, \bar{x}_{21}, \bar{x}_{22}, \bar{x}_{23}, \bar{x}_{24})$ presents the estimated states of the lateral flight control system using the method in Trinh and Huong (2018). Compared to the method in Trinh and Huong (2018), it can be found that the estimated states in the proposed strategy have the greater tracking ability for the states of this kind of interconnected systems with uncertainties. Fig 2 shows the time responses of observation errors related to states of the lateral flight control system. Especially, $\bar{e} = \text{col}(\bar{e}_{11}, \bar{e}_{12}, \bar{e}_{13}, \bar{e}_{21}, \bar{e}_{22}, \bar{e}_{23}, \bar{e}_{24})$ presents the observation errors related to states of

the lateral flight control system using the strategy in Trinh and Huong (2018). According to Fig 2, compared to the previous approach, the observation errors in the presented strategy are smaller and adjusted to 0 faster, it also demonstrates that this dynamic observer has the great identification ability with small errors for nonlinear interconnected systems with uncertainties. Fig 3 presents time responses of the control laws for the lateral flight control system. The simulation results of the lateral flight control system demonstrate that the proposed dynamic observer is effective.

Conclusion

In this paper, a novel dynamic observer is presented for complex nonlinear interconnected systems with matched and mismatched uncertainties. This dynamic observer can estimate the values of states which can not be accessed in general situation. The proposed method has great identification ability with small estimated state errors for nonlinear interconnected systems with uncertainties. It should be mentioned that the uncertainties of nonlinear interconnected systems have general structures, which means that the proposed method can be effectively used in generalised nonlinear interconnected systems. In the future, the proposed dynamic observer will be combined with some advanced control methods to improve the control performance and the robustness for nonlinear interconnected systems with uncertainties.

Funding

The author(s) disclosed receipt of the following financial support for the research, authorship, and/or publication of this article: This work was supported by Wuxi University Research Start-up Fund for Introduced Talents (2024r026).

References

Abbasi A and Javad P (2018) An unknown input observer-based decentralized fault detection and isolation for a class of large-scale interconnected nonlinear systems. *Transactions of the Institute of Measurement and Control* 40(8): 2599–2606.

Attia MS, Mohamed KB and Naceur BB (2021) A near-optimal decentralized control approach for polynomial nonlinear interconnected systems. *Transactions of the Institute of Measurement and Control* 43(6): 1363–1375.

Chen WH, Yang J, Guo L and Li SH (2015) Disturbance-observer-based control and related methods—an overview. *IEEE Transactions on industrial electronics* 63(2): 1083–1095.

Feydi A, Salwa E, Chaker J and Naceur BB (2019) Decentralized finite-horizon suboptimal control for nonlinear interconnected dynamic systems using sdre approach. *Transactions of the Institute of Measurement and Control* 41(11): 3264–3275.

Ghali S, Abdelaziz B and Salwa E (2020) A decentralized observer-based optimal control for interconnected systems using the block pulse functions. *Transactions of the Institute of Measurement and Control* 42(15): 3063–3075.

Guo HY and Zhang XG (2021) Sampled observer-based adaptive decentralized control for strict-feedback interconnected nonlinear systems. *Journal of the Franklin Institute* 358(11): 5845–5861.

Huong DC (2023) Finite-time boundedness and finite-time stabilization boundedness for nonlinear interconnected systems with atangana-baleanu-caputo fractional derivative. *Transactions of the Institute of Measurement and Control* 45(9): 1738–1746.

Kadrine A, Tir Z, Malik OP, Hamida MA, Reatti A and Houari A (2020) Adaptive nonlinear high gain observer based sensorless speed estimation of an induction motor. *Journal of the Franklin Institute* 357(13): 8995–9024.

Khalil HK (2017) Cascade high-gain observers in output feedback control. *Automatica* 80: 110–118.

Li SZ, Wang HP, Aitouche A and Christov N (2018) Sliding mode observer design for fault and disturbance estimation using Takagi Sugeno model. *European Journal of Control* 44: 114–122.

Liu WJ (2011) Decentralized control design for a class of non-linear large-scale systems with matched and unmatched uncertainties. *Transactions of the Institute of Measurement and Control* 33(5): 631–644.

Mahmud MA, Pota H and Hossain M (2012) Full-order nonlinear observer-based excitation controller design for interconnected power systems via exact linearization approach. *International Journal of Electrical Power & Energy Systems* 41(1): 54–62.

Orihuela L, Roshany-Yamchi S, García RA and Millán P (2017) Distributed set-membership observers for interconnected multi-rate systems. *Automatica* 85: 221–226.

Ortega R, Bobtsov A, Dochain D and Nikolaev N (2019) State observers for reaction systems with improved convergence rates. *Journal of Process Control* 83: 53–62.

Rtibi H, Salwa E and Naceur BB (2019) Development of a decentralized nonlinear controller for a class of uncertain polynomial interconnected systems: Application for a large scale power system. *Transactions of the Institute of Measurement and Control* 41(8): 2236–2249.

Song CC, Wang HP, Tian Y and Zheng G (2021) Event-triggered observer design for output-sampled systems. *Nonlinear Analysis: Hybrid Systems* 43: 101112.

Tlili AS (2019) Proportional integral observer-based decentralized stabilization design scheme for nonlinear complex interconnected systems. *Transactions of the Institute of Measurement and Control* 41(7): 1811–1823.

Trinh H and Huong DC (2018) A new method for designing distributed reduced-order functional observers of interconnected time-delay systems. *Journal of the Franklin Institute* 355(3): 1411–1451.

Trinh H, Huong DC and Saeid N (2019) Observer design for positive fractional-order interconnected time-delay systems. *Transactions of the Institute of Measurement and Control* 41(2): 378–391.

Unal G (2021) Integrated design of fault-tolerant control for flight control systems using observer and fuzzy logic. *Aircraft Engineering and Aerospace Technology* 93(4): 723–732.

Vafaei A and Yazdanpanah MJ (2016) A chain observer for nonlinear long constant delay systems: A matrix inequality approach. *Automatica* 65: 164–169.

Wang TC and Tong SC (2018) Observer-based fuzzy adaptive optimal stabilization control for completely unknown nonlinear interconnected systems. *Neurocomputing* 313: 415–425.

Wu SF, Grimble MJ and Breslin SG (1998) Introduction to quantitative feedback theory for lateral robust flight control systems design. *Control Engineering Practice* 6(7): 805–828.

Yang GT, Barboni A, Rezaee H and Parisini T (2022) State estimation using a network of distributed observers with unknown inputs. *Automatica* 146: 110631.

Yeh YL (2022) Output feedback sliding-mode control based on dynamic-gain observer for non-minimum phase systems. *Journal of the Franklin Institute* .

Zhang ZH, Zhang P and Leifeld T (2022) Reduced-order observer design for fault diagnosis of Boolean control networks. *Automatica* 146: 110618.

Zuo Y, Lai CY and Iyer KLV (2023) A review of sliding mode observer based sensorless control methods for pmsm drive. *IEEE Transactions on Power Electronics* 38(9): 11352–11367.